

# Review of Motion Blur Estimation Techniques

Shamik Tiwari, V. P. Shukla, and A. K. Singh

FET, Mody Institute of Technology & Science, Laxmangarh, India

Email: shamiktiwari@hotmail.com, drsvprasad2k@yahoo.com, ajay.kr.singh07@gmail.com

S. R. Biradar

SDM College of Engineering, Hubli-Dharwad, India

Email: srbiradar@gmail.com

**Abstract**—The goal of image restoration is to improve a given image in some predefined sense. Restoration attempts to recover an image by modelling the degradation function and applying the inverse process. Motion blur is a common type of degradation which is caused by the relative motion between an object and camera. Motion blur can be modeled by a point spread function consists of two parameters angle and length. Accurate estimation of these parameters is required in case of blind restoration of motion blurred images. This paper compares different approaches to estimate the parameters of a motion blur namely direction and length directly from the observed image with and without the influence of Gaussian noise. These estimated motion blur parameters can then be used in a standard non-blind deconvolution algorithm. Simulation results compare the performance of most common motion blur estimation methods.

**Index Terms**—motion blur, hough transform, radon transform, Cepstral transform

## I. INTRODUCTION

Image restoration is one of the fundamental problems in image processing. It aims at reconstruction of true image from the degraded image. There are two main kinds of blurring: one is motion blur, which is caused by the relative motion between the camera and object during image capturing; the other is defocus blur, which is due to the inaccurate focal length adjustment at the time of image capturing. Blurring induces the degradation of image quality, specifically for sharp images where the high frequency information can be easily lost due to blur. An image restoration technique refers as non-blind restoration, if blur kernel information is available. In case of blind restoration, blur kernel information is not known. Blind image restoration problem has been categorized into two groups. In the first group, we can put those methods in which the point spread function (PSF) of blur is estimated in first step and then degraded image is restored using any of the classical deconvolution methods such as wiener or inverse filtering in subsequent step. In the methods of second group, PSF estimation and image restoration are achieved simultaneously. The work

reviewed in this paper falls in the former category where PSF parameters are estimated before image deconvolution.

A variety of methods for the identification of blur parameters have been proposed in literature [1], [2], [3], [4] and [5]. Wavelet transform method is more effective to detect edges than other edge detection techniques. This uses horizontal, vertical and diagonal coefficients at different scale to detect edges. Tong *et al.* [6] proposed a scheme that uses the Harr wavelet transform (HWT) in discriminating different types of edges as well as recovering sharpness from the blurred version, and then determines whether an image is blurred or not and up to what extent if it is blurred. Ratnakar *et al.* [7] presented an approach to estimate the motion blur parameters using Gabor filter for blur direction and radial basis function neural network for blur length with sum of Fourier coefficients as features. Yang *et al.* [8] addressed the motion blur detection scheme using support vector machine (SVM) to classify the digital image as blurred or sharp. Chen *et al.* [9] considered statistics of the natural scenes and utilised multi-resolution decomposition methods to extract motion blur features to train and test probabilistic support vector machine. In Cepstrum domain, motion blur can be separated from blurred image. Cannon's method [1] proposed Cepstrum domain for estimation of motion blur parameters. Krahmer *et al.* [10] used Radon transform for searching characteristics of motion blur in cepstral analysis. Lokhande *et al.* [11] estimated parameters of motion blur using periodic patterns in frequency spectrum. They proposed blur direction identification using Hough transform and blur length estimation by collapsing the 2-D spectrum into 1-D spectrum. Fang *et al.* [12] proposed another method consisting of Hann windowing and histogram equalization as pre-processing steps. They applied Hann windowing to remove boundary artefacts and histogram equalization to improve the contrast of the image. Rekleities [13] used steerable filter to detect the motion blur angle corresponding to maximum response of gradients. Chang *et al.* [2] used bispectrum to detect motion blur parameters. They showed that bispectrum is more invariant to noise in comparison to cepstral. A method using Discrete Cosine Transform (DCT) of image is presented by Yoshida *et al.* [14] to estimate uniform

---

Manuscript received December 13, 2013; revised April 14, 2014.

motion blur parameters. Shamik *et al.* [15] discussed different approaches for motion blur detection and estimation. In the paper, we investigated the performance of uniform motion blur detection and parameter identification methods in presence of noise.

This paper is organized in eight sections including the present section. In section 2 and section 3, we discuss the image degradation model and theory of motion blur estimation respectively. Section 4 is devoted to blur angle estimation approaches and section 5 discusses two methods for motion length estimation. Section 6 presents the simulation results. After estimation of blur parameters, image restoration is carried out in section 7 using Lucy-Richardson approach. In the final section 8, conclusion is discussed. All the implementations are performed in the MATLAB 7.0 environment.

## II. IMAGE DEGRADATION MODEL

The image degradation process can be modelled by the following convolution process [16]

$$g(x, y) = f(x, y) * h(x, y) + \eta(x, y) \quad (1)$$

where,  $g(x, y)$  is the degraded image in spatial domain,  $f(x, y)$  is the uncorrupted original image in the spatial domain,  $h(x, y)$  is the point spread function that caused the degradation and  $\eta(x, y)$  is the additive noise. Since, convolution in spatial domain is equal to the multiplication in frequency domain, (1) can be written as

$$G(u, v) = F(u, v)H(u, v) + N(u, v) \quad (2)$$

In order to develop reliable blur detection, it is essential to understand the image degradation process. Degradation function may be due to improper opening and closing of shutter, atmospheric turbulence, out of focus of lens or due to motion blur. The noise and degradation functions have contradicting effects on the image spectrum. The degradation function gives averaging effect on the image data and behaves like a low pass filter, whereas noise often introduces additive broad band signals in the image data. When an object or the camera is moved during light exposure, a motion blurred image is produced. The motion blur can be in the form of translation, rotation, and sudden change of the scale or some combinations of these forms. When the scene to be recorded translates relative to the camera at a constant velocity ( $v_{\text{relative}}$ ) under an angle of  $\alpha$  radians with the horizontal axis during the exposure interval  $[0, t_{\text{exposure}}]$ , the distortion is one dimensional. Defining the length of motion as  $L = v_{\text{relative}} \times t_{\text{exposure}}$ , the PSF of uniform motion blur in spatial domain can be described as [16]

$$h(x, y) = \begin{cases} \frac{1}{L} & \text{if } \sqrt{x^2 + y^2} \leq \frac{L}{2} \text{ and } \frac{x}{y} = -\tan \alpha \\ 0 & \text{otherwise} \end{cases} \quad (3)$$

The frequency response of  $h$ , is given by

$$H(u, v) = \text{sinc}(\Pi L(u \cos \alpha + v \sin \alpha)) \quad (4)$$

Fig. 1(a) and (b) show an example of motion blur PSF and corresponding OTF with specified parameters. The PSF estimation techniques are applied to estimate two parameters length ( $L$ ) and angle ( $\alpha$ ).

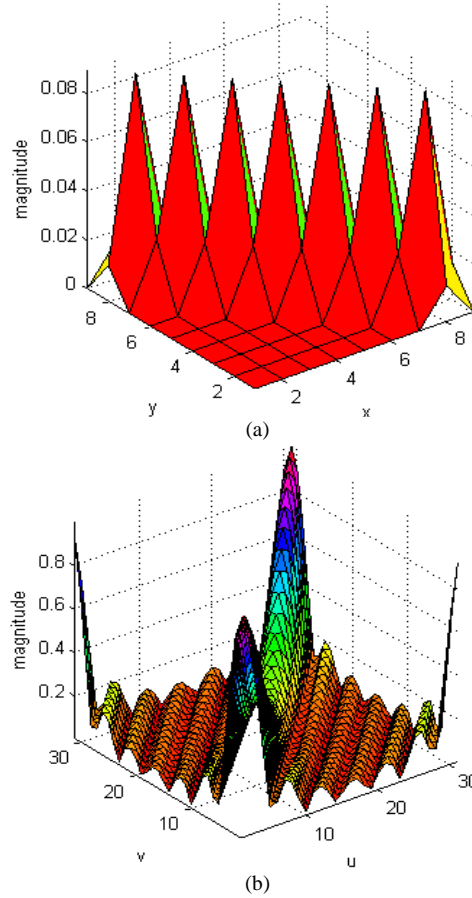


Figure 1. (a) PSF of motion blur with angle  $45^\circ$  and length 10 pixels, (b) OTF of PSF in (a)

## III. ESTIMATION OF MOTION BLUR PARAMETERS

If we transform the uniform motion blurred image in frequency domain, we can extract the motion blur parameters from frequency spectrum. Fig. 2 shows the effect of motion blur on the logarithmic frequency spectrum of original image. Frequency spectrum of motion blurred image shows the dominant parallel lines orthogonal to the motion orientation with very low values near to zero [16]. Therefore, the task of estimating the motion orientation is analogous to the task of calculating orientation of these parallel lines. To find the line direction, we can apply any line fitting method like Radon transform, Hough transform or any other orientation extraction method.

Motion length estimation should take the benefit of the fact that, when motion length increases, the parallel dark lines of the fourier spectrum get closer to each other. For estimating the motion length, we can measure the distance ( $d$ ) between parallel dark lines from each other, then using these distances motion blur length can be predicted.

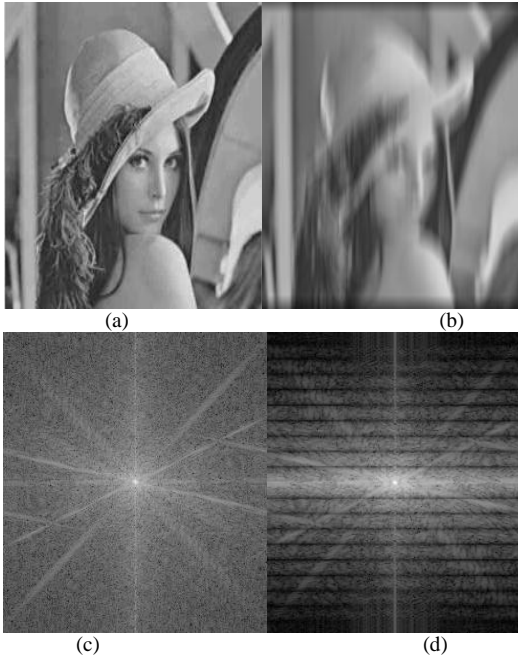


Figure 2. (a) Original image (b) Blurred image with motion length 20 pixels and motion orientation  $90^{\circ}$  (c) Fourier spectrum of original image (d) Fourier spectrum of blurred image

#### IV. MOTION BLUR ORIENTATION ESTIMATION

In this section, we are discussing Hough transform Radon transform and steerable filter methods of motion blur angle estimation in that order.

##### A. Hough Transform Method

The Hough transform [17] can be applied to find global patterns such as lines, circles, and ellipses in an image in a parameter space. It is especially useful in line detection because lines can be easily detected as points in Hough transform space, based on the polar representation of line given by

$$\rho = x \cos \theta + y \sin \theta \quad (5)$$

where  $(x, y)$  are cartesian coordinates of a point on the line;  $\theta$  is the angle between the perpendicular from the origin to the given line and the x-axis and  $\rho$  is the length of the perpendicular. Thus, a pair of coordinates  $(\rho, \theta)$  can describe a line in polar domain. Fig. 3 shows transformation of line parameters from image domain to polar domain.

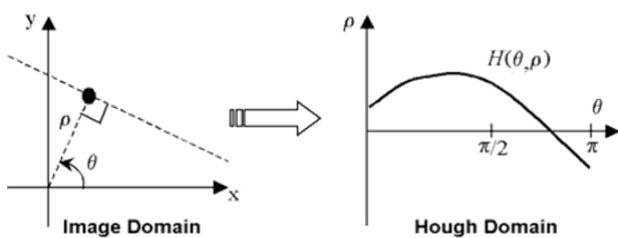


Figure 3. Hough transform

The Hough transform based PSF estimation for motion blurred images using the log spectrum of the blurred images discussed in [11]. The authors illustrated the idea

of motion blur direction estimation by arguing that the spectrum of a sharp image has isotropic nature whereas a motion blurred image has anisotropic nature. Therefore, the spectrum of a motion blurred image is expected to be biased in a direction perpendicular to the direction of blur. The Hough transform is used to obtain the accumulator array from the edge map of log spectrum image.

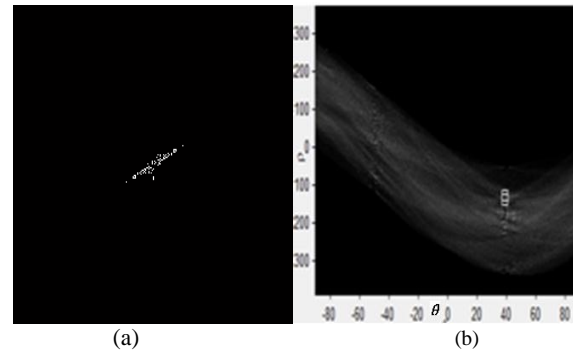


Figure 4. (a) Edge map of cepstral of fig.1(a) blurred with motion length 10 pixels and motion orientation  $60^{\circ}$  (b) Hough transform of (a)

The blur direction is obtained by locating the maximum value of this accumulator array. The  $\theta$  value corresponding to the maximum value of the accumulator array is the angle perpendicular to the blur direction. True blur direction is given by  $90^{\circ} - \theta$ . Fig. 4 shows the result of applying Hough transform to the edge map of cepstral transform of an image, which was degraded by a linear motion blur of length 10 pixels and orientation  $60^{\circ}$ . Peak in Hough transform corresponds to the motion blur angle. Algorithm-1 gives the steps for motion blur angle estimation using Hough transform method.

##### Algorithm1: Motion Blur Angle Estimation

1. Convert blurred RGB image  $f(x, y, 3)$  to gray level image  $f(x, y)$ .
2. Perform Hann windowing over the image to remove boundary artefacts.
3. Compute the Fourier transform  $F(u, v)$  of step2 image.
4. Compute the log spectrum of  $F(u, v)$ .
5. Compute the inverse Fourier transform of log spectrum.
6. Find the edge map of the cepstral of step 5.
7. Let  $\alpha_{min}$  and the  $\alpha_{max}$  be the minimum and maximum values of the motion blur angle.
8. Initialize the accumulator array  $A(r, \alpha)$  to zero.
9. Repeat for each edge point  $(x_i, y_i)$

$$\begin{aligned} & \text{Repeat for } \alpha = \alpha_{min} \text{ to } \alpha_{max} \\ & \{ \\ & \quad r = x_i \cos \alpha + y_i \sin \alpha \\ & \quad A(r, \alpha) = A(r, \alpha) + 1 \\ & \quad \alpha = \alpha + 1 \\ & \} \end{aligned}$$

10. Find the peak in Hough transform (the maximum value in accumulator array) which is perpendicular to the motion blur angle.

##### B. Radon Transform Method

Radon transform [17] is competent to transform two dimensional images with lines into a domain of possible

line parameters  $\theta$  and  $\rho$ , which have the same meaning as given in above section. Each line in the image will give a peak positioned at the corresponding line parameters. It computes the projections of an image matrix along specified directions. A projection of a two-dimensional function  $f(x, y)$  is a set of line integrals. The Radon function computes the line integrals from multiple sources along parallel paths, or beams, in a certain direction.

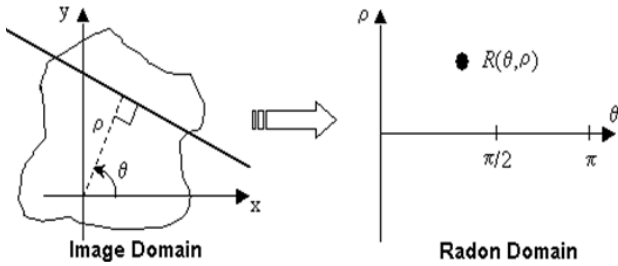


Figure 5. Radon Transform

An arbitrary point in the projection expressed as ray-sum along the line  $x \cos \theta + y \sin \theta = \rho$  is given by discrete domain equation as  $g(\rho, \theta)$

$$= \sum_{x=0}^{M-1} \sum_{y=0}^{N-1} f(x, y) \delta(x \cos \theta + y \sin \theta - \rho) \quad (6)$$

where  $\delta(\cdot)$  is delta function. The advantage of Radon transform over other line fitting algorithms, such as Hough transform and robust regression, is that we do not need to specify edge pixels of the lines. Fig. 5 shows the transformation of image domain to a Radon domain. To find direction of parallel lines of spectrum, first compute the Radon transform  $R$  of an image, and then the position of high spots along the  $\theta$  axis of  $R$  shows the motion direction. Fig. 6 shows the result of applying Radon transform to the logarithmic frequency spectrum of an image. The peak in Radon transform corresponds to the motion blur angle [18]. Algorithm-2 gives the steps for motion blur angle estimation using Radon transform method.

**Algorithm2: Motion Blur Angle Estimation**

1. Convert blurred image  $f(x, y, 3)$  to gray level image  $f(x, y)$ .
2. Perform Hann windowing over  $f(x, y)$  to remove boundary artifacts.
3. Compute the Fourier transform  $F(u, v)$  of step2 image.
4. Compute the log spectrum of  $F(u, v)$ .
5. Repeat for  $\alpha = 0$  to 180
  - Repeat for  $u = 0$  to  $M-1$
  - Repeat for  $v = 0$  to  $N-1$
  - {
  - $\rho = u \cos \alpha + v \sin \alpha$
  - $g(\rho, \alpha) = g(\rho, \alpha) + g(\rho, \alpha) \delta(u \cos \alpha + v \sin \alpha - \rho)$
  - }
6. Find the peak in Radon transform matrix array which is corresponding to the motion blur angle.

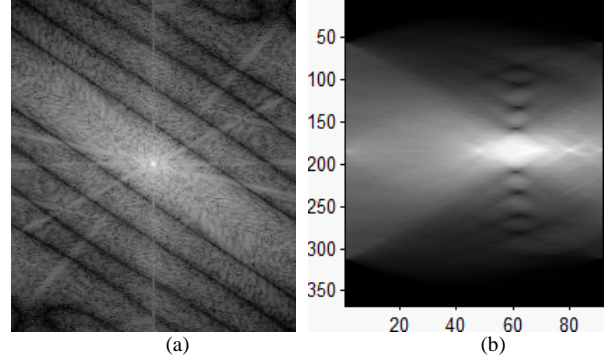


Figure 6. (a) Fourier spectrum of figure 1(a) Blurred with motion length 10 pixels and motion orientation  $60^\circ$  (b) Radon transform of (a)

**C. Steerable Filters Method**

Steerable filters fundamentally offer directional edge detection since they act as band-pass filters in a particular orientation [13]. The edge located at different orientations in an image can be detected by splitting the image into orientation sub-bands obtained by basis filters having these orientations. As we discussed in earlier sections, the power spectrum of the blurred image is characterized by a central ripple that goes across the direction of the motion. In order to extract this orientation, we treat the power spectrum as an image and a linear filter is applied so it could identify the orientation of the ripple. More specifically the second derivative of a two dimensional Gaussian is used. If we filter the power spectrum of a blurred image with second derivative of the Gaussian along the x-axis, we can extract maximum response when the ripple is across the x-axis. In order to extract the orientation of the ripple, we have to find the angle  $\theta$  in which the filters of the second derivative of a Gaussian oriented at that angle  $\theta$  is going to give the highest response. The second derivative of the Gaussian filter belongs to a family of filters called steerable filters, whose response can be calculate at any angle  $\theta$  based only on the responses of basis filters.

The second derivative of the Gaussian filter belongs to a family of filters called steerable filters, whose response can be calculate at any angle  $\theta$  based only on the responses of basis filters. A steerable filter can be given in any arbitrary orientation by its interpolation functions. For every feasible angle the filter is convolved with the spectrum of the image. The response with the highest  $L_2$  norm indicates the blur angle. The three basis filters are defined by

$$G_{2a} = 0.921(2x^2 - 1)e^{-(x^2+y^2)} \quad (7)$$

$$G_{2b} = 1.843 xy e^{-(x^2+y^2)} \quad (8)$$

$$G_{2c} = 0.921(2y^2 - 1)e^{-(x^2+y^2)} \quad (9)$$

where  $G_2$  represents the second derivative of a Gaussian. The interpolation functions  $k$  are given by

$$k_a(\theta) = \cos^2(\theta) \quad (10)$$

$$k_b(\theta) = -2\sin(\theta)\cos(\theta) \quad (11)$$

$$k_c(\theta) = \sin^2(\theta) \quad (12)$$

And the steerable filter is obtainable as

$$RG_2^\theta = k_a(\theta)RG_{2a} + k_b(\theta)RG_{2b} + k_c(\theta)RG_{2c} \quad (13)$$

where RG is the response of the filter.

Algorithm-3 gives the steps for motion blur angle estimation using Radon transform method.

**Algorithm3: Motion Blur Angle Estimation**

1. Convert blurred image  $f(x,y,3)$  to gray level image  $f(x,y)$ .
2. Perform Hann windowing over  $f(x,y)$  to remove boundary artifacts.
3. Compute the Fourier transform  $F(u,v)$  of step2 image.
4. Compute the power spectrum of  $F(u,v)$ .
5. Repeat for  $\alpha = 0$  to 180
  - { Apply steerable filters with orientation  $\alpha$  to power spectrum.
  - Calculate the mean of filter output.
  - }
6. Find the angle for which we have max mean value which is corresponding to the motion blur angle.

**V. MOTION BLUR LENGTH ESTIMATION**

In this section we are discussing Radon transform and 1-D Cepstral methods of motion blur length estimation.

**A. Radon Transform Method**

As explained in section IV, Radon transform computes the projection of an image along specified directions. The blur length estimated after obtaining the blur direction using any one of the discussed approaches. Firstly the log spectrum of blurred image is projected to x-axis by Radon transform with estimated angle. The local minima correspond to the dark lines separated with almost identical distance (d). Fig. 7 illustrates this concept. Detecting those minima and averaging the distances between them, we can compute the final blur length [19].

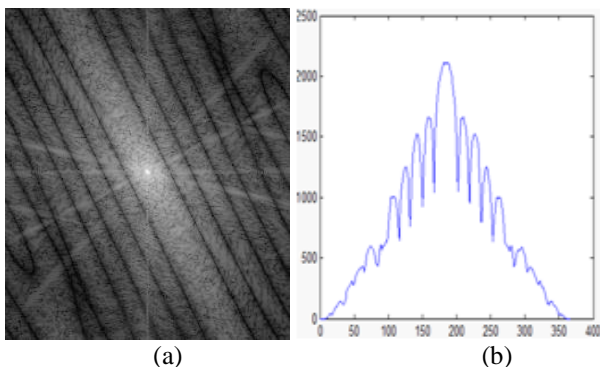


Figure 7. (a) Fourier spectrum of image in Fig. 1(a) blurred with motion length 15 pixels and motion orientation  $30^\circ$  (b) Radon transform at the angle  $30^\circ$

Algorithm-4 gives the steps for motion blur angle estimation using Radon transform method.

**Algorithm4: Motion Blur Length Estimation**

1. Convert blurred image  $f(x,y,3)$  to gray level image  $f(x,y)$ .
2. Perform Hann windowing over the image  $f(x,y)$  to remove boundary artifacts.
3. Compute the Fourier transform  $F(u,v)$  of step2 image.
4. Compute the log spectrum of  $F(u,v)$ .
5. Find the Radon transform of the log spectrum at the estimated angle.
6. Detect the all local minima in radon transform and average the distance between them as d.
7. For an image of size  $N \times N$  motion length is given by  $N/d$ .

**B. Cepstral Method**

Cepstrum transform [1] can be used for separation of blur components and image components. Cepstrum transform of an image  $f(x,y)$  is defined as follows:

$$C\{f(x,y)\} = F^{-1}(\log |F(f(x,y))|) \quad (14)$$

Uniform motion blur in Frequency domain has periodic patterns by zero crossing of sinc function. Periodic patterns make negative peaks in cepstrum domain. Fig. 11 shows cepstrum of blurred image has the negative peaks that are arisen by motion blur. For an estimated angle from section IV, we can estimate the blur length in an image. With the image in the cepstrum domain, first rotate the image by the expected blur angle and then take the average of each column to collapse 2-D cepstral into 1-D. By finding the number of columns between origin and first negative peak, we are able to find the periodicity and estimate the blur length for a given angle. Fig. 8 illustrates this concept. Algorithm-5 gives the steps for motion blur angle estimation using Radon transform method.

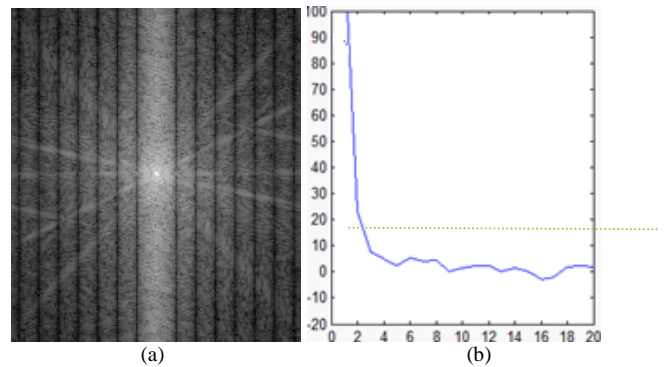


Figure 8. (a) Fourier spectrum of figure 1(a) blurred with motion length 15 pixels and motion orientation  $0^\circ$  (b) 1-D cepstrum of (a)

**Algorithm5: Motion Blur Length Estimation**

1. Convert blurred image  $f(x,y,3)$  to gray level image  $f(x,y)$ .
2. Perform Hann windowing over the image  $f(x,y)$  to remove boundary artifacts.
3. Compute the Fourier transform  $F(u,v)$  of step2 image.
4. Compute the log spectrum of  $F(u,v)$ .
5. Compute the inverse Fourier transform of log spectrum.
6. Rotate the cepstral by the estimated angle in the inverse direction.

7. Convert the 2-D matrix of step 6 to 1-D by taking the averages of columns.
8. Find the distance of first negative peak from the origin which is corresponding to motion length.

VI. RESULT ANALYSIS

To simulate motion blur estimation approaches, we have degraded Cameraman image of size (256×256) artificially with varying degree of motion blur parameters. Images are contaminated by different types of noise. Most common types of noise are impulsive and Gaussian noise, which affect the image at the time of acquisition due to noisy sensors. Noise also contaminates the image during transmission due to channel errors. Although there are different noise models, this work confines to dealing with blur in the occurrence of Gaussian noise which is the most common scenario in practical applications. The Gaussian noise model is expressed as

$$\eta(x, y) = \frac{1}{2\pi\sigma^2} e^{-\left(\frac{x^2+y^2}{2\sigma^2}\right)} \quad (15)$$

It is characterized by its variance term  $\sigma^2$ .

In order to examine the robustness of these parameter estimation methods in presence of noise additive Gaussian noise of 40db signal to noise ratio (SNR) is added to create noisy blurred images. To examine angle estimation methods discussed in section IV, we have degraded image with angles in the range [0, 90] degree with step size 5° and fixed blur length of 15 pixels. Fig. 9 presents the plot of absolute errors between actual and predicted blur angles. Fig. 10 gives the absolute errors between actual and predicted blur angles in presence of noise. To inspect accuracies of length estimation methods presented in section V, we have degraded image with different lengths in the range [5, 20] pixels and fixed blur angle 0°. Fig. 11 presents the absolute errors between actual and predicted blur lengths. Fig. 12 gives the absolute errors between actual and predicted blur lengths in presence of noise. It is obvious from these plots that noise degrades the performance of these methods badly.

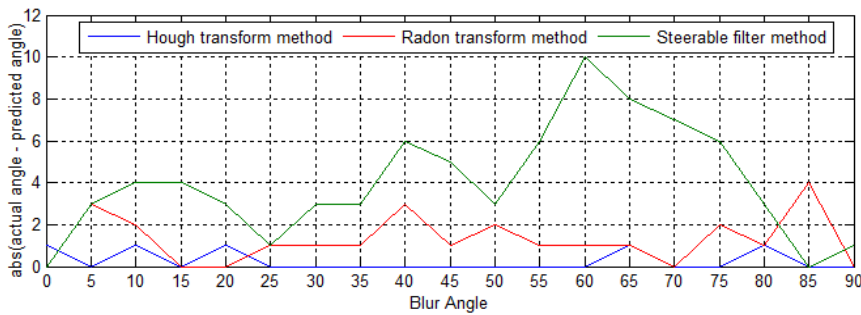


Figure 9. Motion blur angle estimation with blur length 15 pixels

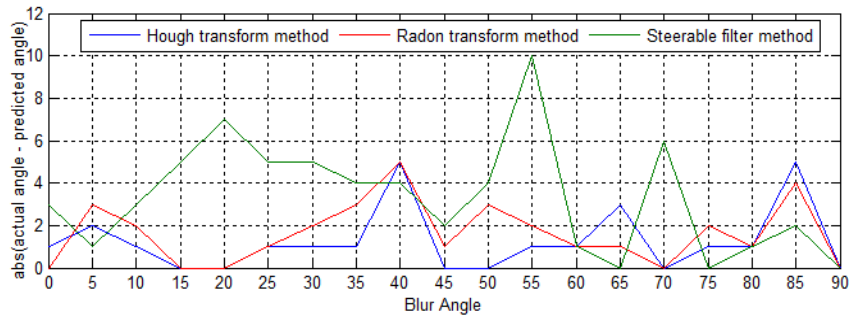


Figure 10. Motion blur angle estimation with blur length 15 pixels and 40db Gaussian noise

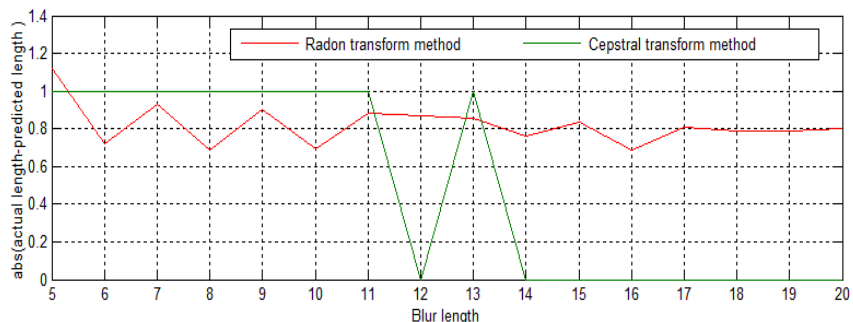


Figure 11. Motion blur length estimation with blur angle 0°

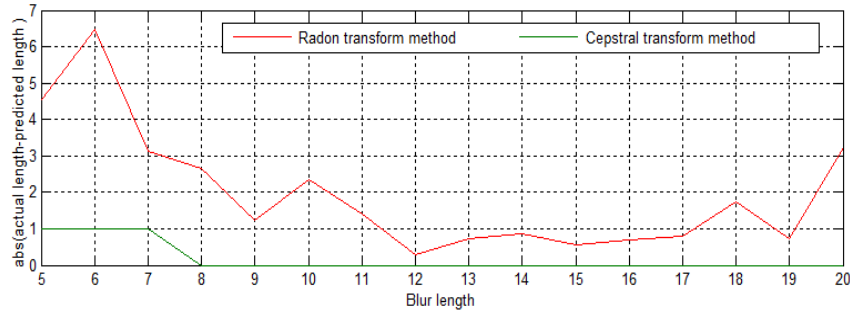


Figure 12. Motion blur length estimation with blur angle 0° and 40db Gaussian noise.

To carry out extensive comparative study, simulation has been carried out on fifteen standard images including Cameraman, Lena, Tree, Barbara, Baboon etc. of size (256 × 256), that were degraded by different orientations and lengths of motion blur. For motion blur angle estimation, we have degraded these images with varying angles in the range [0, 90] degree with step size 5° and fixed blur length of 15 pixels. For motion blur length estimation, we have degraded these images with varying lengths in the range [5, 20] pixels with step size 1 and fixed blur orientation 0°. Table I and III present the results of various approaches for angle and length estimation. Table II and IV present the results of various approaches for angle and length estimation in noisy blurred images. In these tables, the columns named “angle tolerance” and “length tolerance” illustrate the absolute value of errors (i.e. difference between the real values and the estimated values of the angle and length), respectively.

TABLE I. SIMULATION RESULTS BLUR ANGLE ESTIMATION ALGORITHMS ON WITH BLUR LENGTH 10 PIXELS

Cases	Angle tolerance(in degree)		
	Blur Length L=15		
	Hough transform method	Radon transform method	Steerable filter method
Best estimate	0	0	0
Worst estimate	1	4	10
Average estimate	0.2632	1.2632	2.9
RMSE	0.5130	1.6859	4.7793
NRMSE	0.0161	0.0408	0.0955

To examine the accuracy of these methods in estimating motion blur parameters, we used mean absolute error (MAE), root mean square error (RMSE) and normalized root mean square error (NRMSE) statistical measures. RMSE and NRMSE are calculated by (16) and (17) respectively.

$$E_{rmse} = \sqrt{\frac{\sum(T - Y)^2}{N}} \quad (16)$$

$$E_{nrms} = \sqrt{\frac{\sum(T - Y)^2}{\sum(T - \bar{T})^2}} = \sqrt{\frac{Var(E)}{Var(T)}} \quad (17)$$

where T is target vector, Y is estimated vector,  $\bar{T}$  represents mean of target vector and N is the number of

results. NRMSE is the square root of the variance of the error over the variance of the target pattern. This measure gives values between zero and infinity, where zero represents perfect fit and infinity represents random fit.

TABLE II. SIMULATION RESULTS BLUR ANGLE ESTIMATION ALGORITHMS WITH BLUR LENGTH 10 PIXELS IN PRESENCE OF 40 DB NOISE

Cases	Angle tolerance(in degree)		
	Blur Length L=15		
	Hough transform method	Radon transform method	Steerable filter method
Best estimate	0	0	0
Worst estimate	5	5	10
Average estimate	1.2632	1.6316	3.3158
RMSE	1.9467	2.1643	4.2115
NRMSE	0.0541	0.0519	0.0948

TABLE III. SIMULATION RESULTS BLUR LENGTH ESTIMATION ALGORITHMS

Cases	Length tolerance(in pixels)	
	Blur Angle $\theta=0^\circ$	
	Cepstral transform method	Radon transform method
Best estimate	0	0
Worst estimate	1	1
Average estimate	0.1875	0.8202
RMSE	0.4330	0.8273
NRMSE	0.0847	0.0234

TABLE IV. SIMULATION RESULTS BLUR LENGTH ESTIMATION ALGORITHMS IN PRESENCE OF 40DB NOISE

Cases	Length tolerance(in pixels)	
	Blur Angle $\theta=0^\circ$	
	Cepstral transform method	Radon transform method
Best estimate	0	0
Worst estimate	1	6
Average estimate	0.500	1.9616
RMSE	0.7071	2.5655
NRMSE	0.1085	0.3587

It is evident from the results in Table I and Table II that Hough transform results are more accurate in comparison to other methods for motion blur angle identification. Results in Table III and Table IV show that cepstral method is better than radon transform method for blur length estimation.

### VII. BLURRED IMAGE RESTORATION

A significant application of blur-kernel identification is image reproduction. Estimated blur PSF can be used to deblur an image. Many methods such as Wiener filter and inverse filter. The Lucy-Richardson (L-R) algorithm was developed independently by [20] and [21] and is a nonlinear and basically non-blind method, meaning the PSF, or at least a very good estimate, must be a priori known. The L-R has been derived from Bayesian probability hypothesis where image information is measured to be random quantities that are assumed to have a certain possibility of being formed from a family of other possible random quantities. The difficulty regarding the likelihood that the predictable true image, after convolution with the PSF, is in fact identical with the blurred input image, except for noise, is formulated as a so-called likelihood function, which is iteratively maximized. The solution of this maximization requires the convergence of:

$$\hat{f}(x, y)_{t+1} = \hat{f}(x, y)_t \left[ \frac{h(-x, -y) * \frac{g(x, y)}{h(x, y) * \hat{f}(x, y)}}{h(x, y) * \hat{f}(x, y)} \right] \quad (18)$$

where  $t$  denotes the  $t$ -th iteration. It has the division by  $\hat{f}$  that constitutes the algorithm's nonlinear nature. The image estimate is assumed to contain Poisson distributed noise which is appropriate for photon noise in the data whereas additive Gaussian noise, typical for sensor read-out, is ignored. In order to reduce noise amplification, which is a general problem of maximum likelihood methods, it is common practice to introduce a dampening threshold below which further iterations are (locally) suppressed. Otherwise high iteration numbers introduce artefacts to originally smooth image regions. Fig. 13(c) and (d) show the restoration result of 'cameraman.tif' image using L-R method. It is evident from the figures that restoration algorithms show poor results in case of badly estimated parameters.

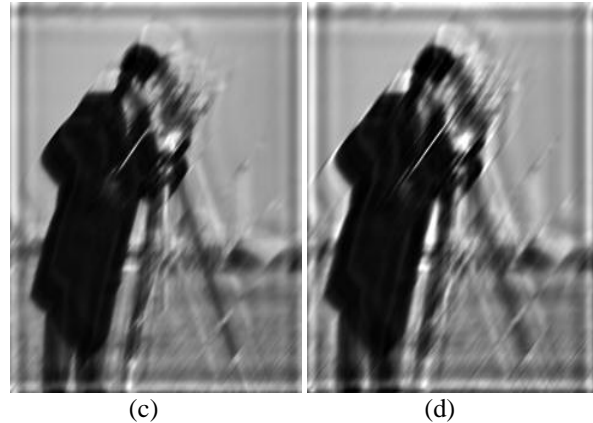
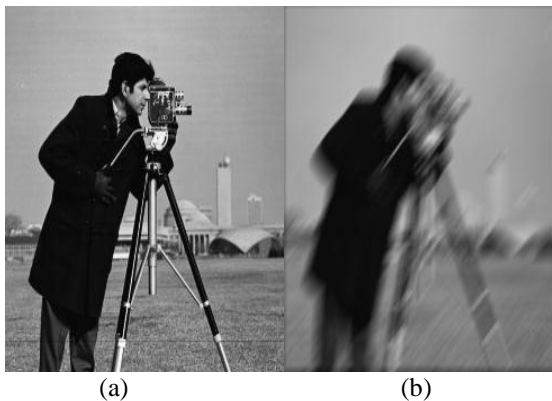


Figure 13. (a) Original image (b) Blurred image with motion length 20 pixels and motion orientation 45° (c) Restored image with true parameters (d) Restored image poorly estimated parameters

### VIII. CONCLUSION

In this paper, we give an overview of some of the most widely used motion blur estimation methods with a quantitative evaluation. When noise is added to a degraded image, the sharpness of edges changes and the parallel dark lines in frequency spectrum of blurred image become fragile or disappear. Motion blur orientation estimation algorithms discussed in section IV shows that the presence of additive Gaussian noise mean absolute error increases from 0.2631 to 1.2632, 1.2632 to 1.6316 and 2.9 to 3.3158 for Hough transform, Radon transform and steerable filter methods respectively. In existence of the same noise, the mean absolute error in length estimation for cepstral transform and Radon transform methods increases from 0.1875 to .5 and 0.8202 to 1.9616 respectively. Results of section VII shows that in case of inaccurate estimation of blur model, the image will be rather distorted much more than restored. This work encourages us to design a robust method for motion blur estimation.

### ACKNOWLEDGEMENT

We highly appreciate Faculty of Engineering & Technology, Mody Institute of Technology & Science University, Laxmangarh for providing facility to carry out this research work.

### REFERENCES

- [1] M. Cannon, "Blind deconvolution of spatially invariant image blurs with phase," *IEEE Trans. Acoust. Speech Signal Processing*, vol. 24, no. 1, pp. 56-63, 1976.
- [2] M. M. Chang, A. M. Tekalp, and A. T. Erdem, "Blur identification using the bispectrum," *IEEE Trans. Signal Processing*, vol. 39, no. 10, pp. 2323-2325, 1991.
- [3] Y. S. Chen and I. S. Choa, "An approach to estimating the motion parameters for a linear motion blurred image," *IEICE Trans. Inf. Syst.*, vol. E83-D, no. 7, pp. 1601-1603, 2000.
- [4] D. G. Childers, "The Cepstrum: A guide to processing," *Proceedings of the IEEE*, vol. 65, no. 10, pp. 1428-1443, 1977.
- [5] R. Fabian and D. Malah, "Robust identification of motion and out-of-focus blur parameters from blurred and noisy images," *CVGIP: Graphical, Models and Image Processing*, vol. 53, pp. 403-412, 1991.
- [6] H. Tong, M. Li, H. Zhang, and C. Zhang, "Blur detection for digital images using wavelet transform," in *Proc. IEEE*

*International Conference on Multimedia and Expo*, vol. 1, pp. 17-20, 2004.

- [7] R. Dash, P. K. Sa, and B. Majhi, "RBFN based motion blur parameter estimation," in *Proc. IEEE International Conference on Advanced Computer Control*, Singapore, Jan 2009, pp. 327-331.
- [8] K. C. Yang, C. C. Guest, and P. Das, "Motion blur detecting by support vector machine," *Proceedings SPIE*, pp. 5916-59160R, 2005.
- [9] M. J. Chen and A. C. Bovik, "No-reference blur assessment using multi-scale gradient," in *Proc. 1st International Workshop on Quality of Multimedia Experience*, San Diego, California, 2009.
- [10] F. Kraemer, Y. Lin, B. McAdoo, K. Ott, J. Wang, D. Widemann, and B. Wohlberg, "Blind image deconvolution: Motion blur estimation" *Tech Rep.*, Univ. Minnesota, 2006.
- [11] R. Lokhande, K. V. Arya, and P. Gupta, "Identification of blur parameters and restoration of motion blurred images," in *Proc. ACM Symposium on Applied Computing*, 2006, pp. 301-305.
- [12] X. Y. Fang, H. Wu, Z. B. Wu, and B. Luo, "An improved method for robust blur estimation," *Information Technology Journal*, vol. 10, pp. 1709-1716, 2011.
- [13] I. M. Rekleities, "Steerable filters and cepstral analysis for optical flow calculation from a single blurred image," in *Proc. the Vision Interface Conference*, Toronto, Ontario, Canada, May 1996, pp. 159-166.
- [14] Y. S. Yoshida, K. Horiike, and K. Fujita, "Parameter estimation of uniform image blur using dct," *IEICE Trans. Fundamentals*, vol. E76, no. 7, pp. 1154-1157, July 1993.
- [15] S. Tiwari, A. K. Singh, and V. P. Shukla, "Certain investigations on motion blur detection and estimation," in *Proc. International Conference on Signal, Image and Video Processing, IIT Patna*, Jan. 2012, pp. 108-114.
- [16] S. Tiwari, V. P. Shukla, S. R. Biradar, and A. K. Singh, "Texture features based blur classification in barcode images," *I. J. Information Engineering and Electronic Business*, MECS Publisher, vol. 5, pp. 34-41, 2013.
- [17] R. C. Gonzalez and R. E. Woods, *Digital Image Processing*, Prentice Hall, 2007.
- [18] M. E. Moghaddam and M. Jamzad, "Linear motion blur parameter estimation in noisy images using fuzzy sets and power spectrum images," *EURASIP Journal on Advances in Signal Processing*, vol. 2007, pp. 1-9, 2007.
- [19] M. Dobeš, L. Machala, and T. Fürst, "Blurred image restoration: A fast method of finding the motion length and angle," *Digital Signal Processing*, vol. 20, no. 6, pp. 1677-1686, 2010.
- [20] W. H. Richardson, "Bayesian-based iterative method of image restoration," *J. Opt. Soc. Am.*, vol. 62, no. 1, pp. 55-60, 1972.
- [21] L. Lucy, "An iterative technique for the rectification of observed distributions," *Astron. J.*, vol. 79, pp. 745-752, 1974.



**Shamik Tiwari** has received his B.E. (Computer Sc. & Engineering) in 2003, M.Tech. (Computer Sc. & Engg.) in 2007 from RGPV University Bhopal and Dr. B. R. Ambedkar University Agra respectively. He has joined as an Asst. Professor in Mody Institute of Technology & Science, Deemed University Laxmangarh in 2009. Presently, he is pursuing Ph.D. in Computer Sc. & Engg. from the MITS Lakshmanagarh. He has published over 25 papers in refereed journals and conference

proceedings. He is an author of the book "Digital Image Processing" from Dhanpat Rai Publishing (India), His current research interest includes digital image processing, pattern classification, and their applications in computer vision.



**Vidya Prasad Shukla** was born in India, in 1954. He received his M.Sc. (Applied Mathematics) in 1976, Ph.D. (Modelling and Computer Simulation) in 1982 and PG Dip. (Computational Hydraulic Engineering) in 1986 from Avadh University Faizabad, Indian Institute of Technology Kanpur and International Institute of Environmental & Hydraulic Engineering (Delft) the Netherlands respectively. He worked and officiated at various posts as Senior Research Officer, Chief Research Officer and HOD Computer Division from Central Water and Power research Station (CWPRS), Pune from 1982 to 2003. Thereafter, he worked as a Professor in BIT, Sathyamangalam and NIT Durgapur. He has joined as a Professor in Mody Institute of Technology & Science, Deemed University Laxmangarh in 2009. He has published over 57 papers in refereed journals and conference proceedings and written 29 technical reports on various clients sponsored research projects of international/national importance. He is an editor of the book "Development of Coastal Engineering" from CWPRS, Pune. His current research interest includes Computer Simulation & Modelling, Image processing, Cellular Automata, Soft-Computing, Computer Vision, Nanotech-simulation, Operations Research, Mathematical Biology, Modelling of Arms Race of Nations.



**Mr. S. R. Biradar** is a Professor in the department of Computer Science and Engineering, SDM, Dharwad, India. He received his B.E, M.Tech and Ph.D. degrees in Computer Science and Engineering from Karnataka University, MAHE Manipal and Jadavpur University respectively. His research interest includes Mobile Ad-hoc networking, advanced wireless communication. He has published over 45 papers in refereed journals and conference proceedings. His current research interest includes Image Processing, Mobile ad hoc networks, and sensor networks.



**Ajay Kumar Singh** was born in India, in 1980. He received his B.E. (Computer Sc. & Engineering) in 2001, M.Tech. (Information Technology) in 2006 from CCS University Meerut and AAI Deemed University Allahabad respectively. He has joined as an Asst. Prof. in Mody Institute of Technology & Science, Deemed University Laxmangarh in 2009. Presently, he is pursuing Ph.D. in Computer Sc. & Engg. from the MITS Lakshmanagarh. He has published over 20 papers in refereed journals and conference proceedings. His current research interest includes Image Processing, Image classification and their applications in computer vision.